DNA double-strand break repair pathway choice in *Dictyostelium*

Duen-Wei Hsu*, Rhian Kiely*, C. Anne-Marie Couto, Hong-Yu Wang, Jessica J. R. Hudson‡, Christine Borer, Catherine J. Pears§ and Nicholas D. Lakin§

Department of Biochemistry, University of Oxford, South Parks Road, Oxford OX1 3QU, UK

*These authors contributed equally to this work
‡Present address: Genome Damage and Stability Centre, University of Sussex, Falmer, Brighton, East Sussex BN1 9RQ, UK
§Authors for correspondence (catherine.pears@bioch.ox.ac.uk; nicholas.lakin@bioch.ox.ac.uk)

Accepted 20 January 2011
Journal of Cell Science 124, 1655-1663

doi:10.1242/jcs.081471

Summary

DNA double-strand breaks (DSBs) can be repaired by homologous recombination (HR) or non-homologous end joining (NHEJ). The mechanisms that govern whether a DSB is repaired by NHEJ or HR remain unclear. Here, we characterise DSB repair in the amoeba *Dictyostelium*. HR is the principal pathway responsible for resistance to DSBs during vegetative cell growth, a stage of the life cycle when cells are predominantly in G2. However, we illustrate that restriction-enzyme-mediated integration of DNA into the *Dictyostelium* genome is possible during this stage of the life cycle and that this is mediated by an active NHEJ pathway. We illustrate that Dclre1, a protein with similarity to the vertebrate NHEJ factor Artemis, is required for NHEJ independently of DNA termini complexity. Although vegetative *dclre1*$^{-}$ cells are not radiosensitive, they exhibit delayed DSB repair, further supporting a role for NHEJ during this stage of the life cycle. By contrast, cells lacking the Ku80 component of the Ku heterodimer that binds DNA ends to facilitate NHEJ exhibit no such defect and deletion of *ku80* suppresses the DSB repair defect of *dclre1*$^{-}$ cells through increasing HR efficiency. These data illustrate a functional NHEJ pathway in vegetative *Dictyostelium* and the importance of Ku in regulating DSB repair choice during this phase of the life cycle.

Key words: *Dictyostelium,* Double-strand break repair, Non-homologous end-joining, Homologous recombination

Introduction

Repair of DNA damage is crucial for maintenance of genome integrity. A particularly toxic variety of DNA lesion is the DNA double-strand break (DSB), which can be repaired by two alternative pathways: homologous recombination (HR) or non-homologous end joining (NHEJ). HR uses sequences homologous to the damaged DNA template to facilitate repair in late S and G2 phases of the cell cycle (Branzei and Foiani, 2008). As such, it is considered an accurate mechanism for re-joining DSBs. The initiating step of HR is 5′ to 3′ resection of DNA termini by multiple nuclease activities, including that of the Mre11–Rad50–Nbs1 (MRN) protein complex in conjunction with CtIP, exonuclease I (Exo1) and Dna2 (Raynard et al., 2008). Subsequent recruitment of Rad51 to form a nucleoprotein filament facilitates homology searching and strand invasion. Extension of the 3′ tail by DNA polymerases then occurs using the undamaged homologous sequence as a template and resolution of the resulting structures leads to accurate repair.

In contrast to HR, NHEJ requires no homologous DNA sequences to facilitate repair, but directly processes and re-ligates DNA termini. In vertebrates, NHEJ is the principal pathway by which DSBs are repaired in G1, although it can also function outside this phase of the cell cycle (Beucher et al., 2009; Deckbar et al., 2007; Rothkamm et al., 2003). The first step in NHEJ is recognition of DNA termini by the DNA-end-binding activity of Ku, which serves as a platform to recruit a number of different proteins to DSBs, including the DNA-dependent protein kinase (DNA-PK) catalytic subunit (DNA-PKcs). DNA-PKcs kinase activity is activated upon DNA end binding and phosphorylates a number of substrates in vivo (Jackson, 2002; Meek et al., 2004), in addition to mediating DNA end synapsis to prevent illegitimate re-joining of DNA DSBs (DeFazio et al., 2002). DNA-PK also promotes the interaction of DNA DSBs with Artemis, a protein required for repair of a subset of breaks induced by IR (Riballo et al., 2004). Artemis, in addition to a number of other factors, including variant DNA polymerases and polynucleotide kinase, is thought to process DNA DSBs to make them compatible with ligation (Lieber et al., 2008). Finally, resealing of the break is performed by the DNA ligase IV–XRCC4–XLF protein complex (Mahaney et al., 2009).

Mechanistically, NHEJ is conserved throughout eukaryotes, although the components used to achieve end joining differ between species. Until recently, DNA-PKcs was thought to be conserved only in vertebrates. However, we and others identified core components of the NHEJ pathway in the amoeba *Dictyostelium*, including a functional orthologue of DNA-PKcs (Block and Lees-Miller, 2005; Hsu et al., 2006; Hudson et al., 2005; Muramoto and Chubb, 2008). Other DNA repair factors absent in conventional invertebrate model organisms used to study DNA repair are also conserved in *Dictyostelium*, including components of the Fanconi anaemia (Zhang et al., 2009) and single-strand break repair pathways (Rajawat et al., 2007). Furthermore, *Dictyostelium* are highly resistant to DNA damage, including ionising radiation (Deering, 1968) and UV light (Freim and Deering, 1970). Therefore, understanding how *Dictyostelium* tolerates high levels of genotoxic stress will provide insights into how other organisms become resistant to DNA damage. These observations, in addition to the genetic tractability of *Dictyostelium*, suggest it will be an

Journal of Cell Science

important model organism to study a variety of DNA repair pathways.

Although *Dictyostelium* is a promising model to study DSB repair, how NHEJ and HR contribute to maintenance of genome stability and the relationship between these two pathways at different stages of the *Dictyostelium* life cycle remains unclear. For example, disruption of the *dnapkcs* and *ku80* genes sensitises *Dictyostelium* cells to DNA DSBs and abrogates phosphorylation of the histone variant H2AX following DNA damage (Hudson et al., 2005). However, this phenotype is only evident when DNA damage is administered to germinating spores. By contrast, *dnapkcs* is not required for cells to phosphorylate H2AX or tolerate DSBs during vegetative cell growth, suggesting that other repair pathways predominate, at least as regards cell viability following DNA damage (Hudson et al., 2005). However, Ku and DNA-PKcs have recently been implicated in recovery from DSBs and progression of vegetative *Dictyostelium* through mitosis, suggesting that NHEJ does function in some respect at this stage of the life cycle (Block and Lees-Miller, 2005; Hsu et al., 2006; Hudson et al., 2005; Muramoto and Chubb, 2008). Here, we address these questions by further characterising the relative contributions of HR and NHEJ to DSB repair in vegetative *Dictyostelium*. We illustrate that, although HR is required for resistance of vegetative *Dictyostelium* cells to DSBs, NHEJ is also active during this stage of the *Dictyostelium* life cycle. We identify Dclre1, a protein with similarity to Artemis, as a factor required for NHEJ and show that disruption of this gene results in delayed DSB repair. By contrast, *ku80*$^{-}$ cells exhibit no such defect, but instead resolve DSBs efficiently through an increased ability to perform HR. Taken together, these data demonstrate active HR and NHEJ pathways in vegetative *Dictyostelium*, and identify Ku as a factor that governs DSB repair pathway choice in this organism.

Results

Homologous recombination is required to maintain cell viability following DNA DSBs in vegetative *Dictyostelium*

Dictyostelium ku80^{-} and *dnapkcs*$^{-}$ cells are not sensitive to DSBs during vegetative cell growth (Hudson et al., 2005). Vegetative *Dictyostelium* have no discernable G1, a short S phase and protracted G2 (Muramoto and Chubb, 2008; Weijer et al., 1984). Given that HR is active during late S and G2 phases of the cell cycle in other organisms, these data imply that HR is required for resistance to DSBs in vegetative *Dictyostelium*. The initiating step of HR is DNA end resection through multiple nucleases, including Mre11, Exo1 and Dna2 (Raynard et al., 2008). Therefore, to assess the contribution of HR to DSB repair in *Dictyostelium*, we generated a strain disrupted in the *exo1* gene. Consistent with a requirement for *exo1* in HR, we observe an inability of *exo1*$^{-}$ cells to perform targeted HR at the *cdk8* locus (Fig. 1A). Furthermore, in contrast to cells disrupted in components of the NHEJ pathway, *exo1*$^{-}$ cells display increased sensitivity to DSBs administered during vegetative cell growth compared with parental Ax2 cells (Fig. 1B). These data illustrate a requirement for *exo1* in HR and demonstrate that this pathway is required to maintain cell viability following DSBs administered during this stage of the *Dictyostelium* life cycle.

Restriction-enzyme-mediated integration of DNA into the *Dictyostelium* genome is dependent on NHEJ

Although *ku80*$^{-}$ and *dnapkcs*$^{-}$ cells are not sensitive to DSBs administered during vegetative cell growth, they are sensitive to this variety of DNA damage when germinating from spores (Hudson et al., 2005). *Dictyostelium* spores have been reported to be in G1 phase of the cell cycle (Chen et al., 2004). It is therefore tempting to speculate that this might explain the requirement for NHEJ at this stage of the life cycle. However, accumulating evidence suggests that, similar to vegetative cell cultures, germinating *Dictyostelium* spores are in G2 (MacWilliams et al., 2006; Muramoto and Chubb, 2008; Weijer et al., 1984). Taken together, these data imply that, similar to humans (Beucher et al., 2009; Deckbar et al., 2007; Rothkamm et al., 2003), NHEJ is active during G2 in *Dictyostelium* and therefore might function during vegetative cell growth. To directly test this, we developed an assay to assess NHEJ in vegetatively growing *Dictyostelium*. Rejoining of linear extrachromosomal plasmids containing a selectable marker has been used to assess NHEJ efficiency in yeast and mammalian cells (see Boulton and Jackson, 1996; Fattah et al., 2010; Secretan et al., 2004; Wilson et al., 1999). However, plasmid DNA undergoes recombination events when transformed into *Dictyostelium*, potentially complicating this approach as regards assessing the efficiency of NHEJ (Katz and Ratner, 1988). As an alternative, therefore, we exploited the observation that co-transfection of linear plasmid DNA with the restriction enzyme used to linearise the vector results in stimulation of DNA integration into the genome by restriction-enzyme-mediated integration (REMI) (Kuspa and Loomis, 1992; Schiestl and Petes, 1991). Co-transfection of a *Bam*HI-linearised plasmid DNA with *Bam*HI restriction enzyme results in stimulation of DNA integration into the genome at genomic *Bam*HI sites without loss of DNA end integrity (Fig. 2A) (Kuspa and Loomis, 1992; Schiestl and Petes, 1991). The retention of the *Bam*HI site upon integration, and the fact that vector DNA has limited sequence homology to the *Dictyostelium* genome, suggest that REMI is mediated by direct ligation of DNA termini, most probably through NHEJ. To test this hypothesis, we assessed efficiency of REMI into the genome of *dnapkcs*$^{-}$ and *ku80*$^{-}$ cells. Whereas transfection with *Bam*HI alone

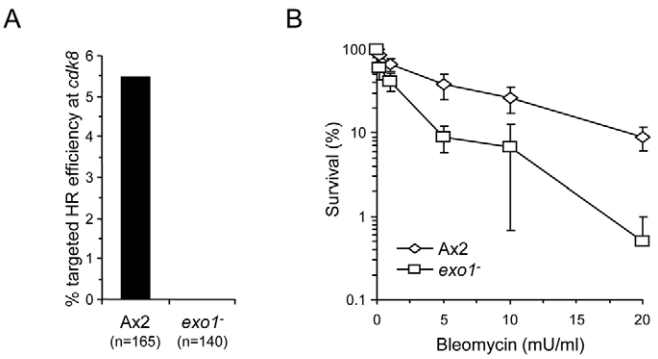

Fig. 1. HR is required for radioresistance in vegetative *Dictyostelium* cells. (**A**) Ax2 or *exo1*$^{-}$ cells were assessed for HR efficiency by measuring targeted integration of the hygromycin cassette at the *cdk8* locus, as described in the Materials and Methods. Multiple transfections were performed and drug-resistant clones were analysed for proper targeting by PCR. The percentage targeted HR efficiency at the *cdk8* locus is calculated as the proportion of aggregate-null colonies against the total number of colonies assessed. The *n* number represents the total number of clones analysed. (**B**) Vegetative Ax2 or *exo1*$^{-}$ cells were exposed to increasing concentrations of bleomycin as indicated and cell viability assessed as described previously (Hudson et al., 2005). Error bars represent the s.e.m. from three independent experiments.

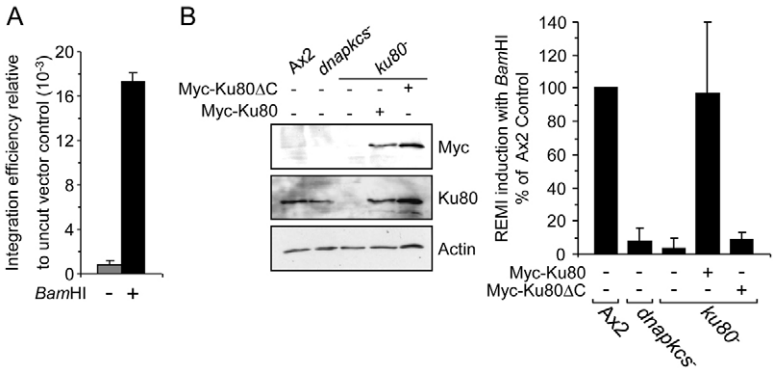

Fig. 2. REMI of plasmid DNA into the genome of *Dictyostelium* is dependent on DNA-PKcs and Ku80. (**A**) REMI of plasmid DNA into the *Dictyostelium* genome. *Bam*HI-linearised plasmids containing a blasticidin-resistant cassette were electroporated into Ax2 in either the presence or absence of *Bam*HI as indicated. In parallel, cells were also transfected with an extrachromosomal vector in either the absence or presence of *Bam*HI. Following selection, the number of blasticidin-resistant colonies was scored. Data are represented as the number of linearised plasmid integrations relative to the number of extrachromosomal vector transformants per 1×10^3 cells. (**B**) REMI of plasmid DNA bearing compatible DNA termini is dependent on NHEJ. Whole-cell extracts were prepared from Ax2 cells or *dnapkcs*$^-$ or *ku80*$^-$ strains containing empty expression vector or vectors driving expression of full-length Myc–Ku80 or Myc–Ku80 lacking the C-terminal 14 amino acid putative DNA-PKcs interaction domain (Myc–Ku80ΔC), and subjected to western blotting using antibodies as indicated (left panel). Cells were electroporated with *Bam*HI-linearised vector containing a blasticidin-resistant cassette either alone or in combination with *Bam*HI. Following selection, blasticidin-resistant colonies were scored for each transfection and REMI efficiency calculated for each strain as fold induction in the number of blasticidin-resistant colonies achieved by addition of *Bam*HI. Data are represented as the percentage induction of a given strain relative to the parental Ax2 strain. Error bars represent s.e.m. from four independent experiments.

does not result in reduced viability of *dnapkcs*$^-$ or *ku80*$^-$ strains (data not shown), REMI efficiency is compromised in *dnapkcs*$^-$ and *ku80*$^-$ cells compared with that of parental Ax2 cells (Fig. 2B). *Dictyostelium* Ku80 contains a C-terminal domain that is conserved only in organisms that contain DNA-PKcs and is required for recruitment of this kinase to DSBs (Falck et al., 2005). Consistent with conservation of this domain in *Dictyostelium*, its deletion results in reduced REMI efficiency similar to that observed in *dnapkcs*$^-$ cells (Fig. 2B). Taken together, these data illustrate that components of the NHEJ pathway are required for REMI of DNA into the *Dictyostelium* genome and provide a convenient assay to assess DNA end joining in this organism.

Identification of a β-CASP-MBL family protein in *Dictyostelium* required for NHEJ

We wished to exploit our REMI assay to characterise other factors required for NHEJ. In particular, given the conservation of DNA-PKcs in *Dictyostelium*, we wanted to assess whether other factors thought to be conserved only in vertebrates function in the NHEJ pathway of this organism. *Dictyostelium* contains a β-CASP (CPSF–Artemis–Smn1–Pso2) metallo-β-lactamase (MBL) (β-CASP-MBL) family nuclease (*dclre1*; DDB_G0277755 at dictybase.org) that has been suggested to be an orthologue of the vertebrate NHEJ nuclease Artemis (also known as SNM1C) (Block and Lees-Miller, 2005; Hsu et al., 2006; Hudson et al., 2005; Muramoto and Chubb, 2008). Artemis possesses 5′ to 3′ exonuclease activity in vitro and, in association with DNA-PKcs, acquires endonuclease activity capable of cleaving 5′ or 3′ single-stranded DNA overhangs or DNA hairpins (Ma et al., 2002; Ma et al., 2005). Therefore, we wished to adapt our assay to assess the ability of cells to process incompatible DNA termini prior to ligation and determine whether Dclre1 is required for these events.

Consistent with a previous report (Kuspa and Loomis, 1992), we observed inefficient REMI when *Bam*HI (5′ overhang) is used in conjunction with plasmid DNA bearing an incompatible 3′ overhang (*Pst*I) at both ends (Fig. 3A; data not shown). However, induction of plasmid integration was achieved when plasmids bearing one compatible (*Bam*HI) and one incompatible (*Kpn*I) 3′ overhang were co-transfected with *Bam*HI (Fig. 3B). REMI was still observed following removal of 5′-terminal phosphate groups by phosphatase treatment prior to introduction of plasmids into cells, illustrating that DNA integration of incompatible DNA ends is not achieved through concatemerisation of plasmids to produce two compatible DNA termini (Fig. 3B). Similar to compatible DNA termini, integration of incompatible DNA ends is dependent on DNA-PKcs and Ku80, illustrating a dependence on NHEJ (Fig. 3C). Therefore, *Dictyostelium* are capable of processing DNA ends to facilitate NHEJ-mediated repair of DSBs.

Next, we tested whether Dclre1 is required for REMI of DNA into the *Dictyostelium* genome. Given the substrate specificity of Artemis in vitro (Ma et al., 2002; Ma et al., 2005), we tested whether Dclre1 is required to process 3′overhang and hairpin DNA structures in vivo by engineering plasmids to contain either a 20-nucleotide 3′ overhang or a hairpin structure at one end. These substrates were employed in REMI alongside plasmids containing two *Bam*HI or *Bam*HI-*Kpn*I ends. All plasmids bearing incompatible DNA ends were capable of undergoing REMI in Ax2 cells, although less efficiently than plasmid DNA with compatible ends (Fig. 3D). REMI was compromised in *dclre1*$^-$ cells, although this was independent of the type of DNA end employed in the assay (Fig. 3D). Therefore, although Dclre1 is required for NHEJ in *Dictyostelium*, its role is independent of DNA termini complexity.

Dclre1 is required for efficient repair of DNA DSBs during vegetative cell growth

The inability of *dclre1*$^-$ cells to perform REMI suggests that NHEJ can function in vegetative *Dictyostelium* cells and contribute to repair of DSBs. However, when we assessed whether Dclre1 is required for resistance to DSBs administered during vegetative cell growth, similar to *ku80*$^-$ and *dnapkcs*$^-$ strains (Hudson et al., 2005),

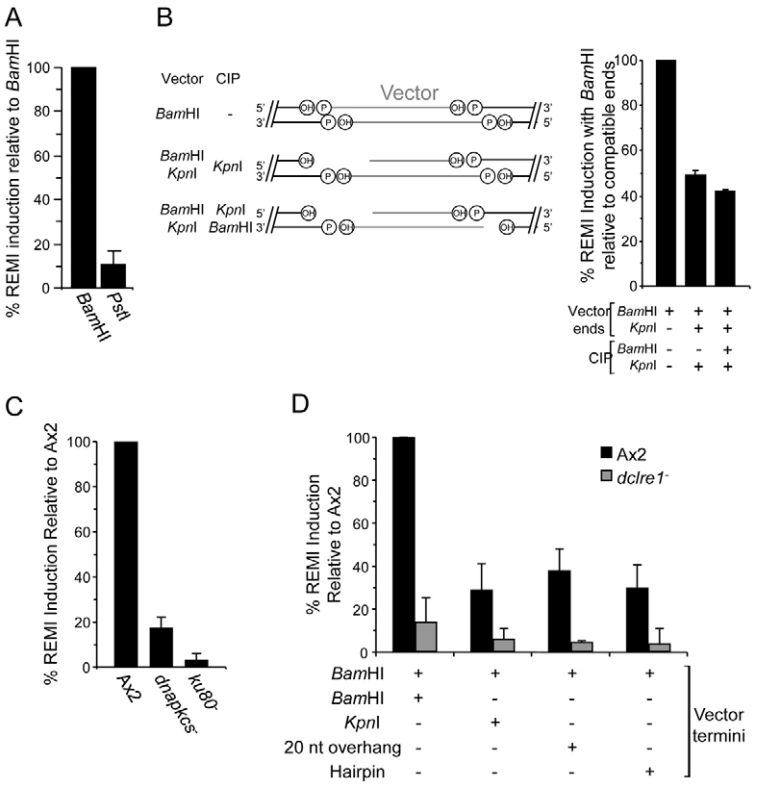

Fig. 3. Dclre1 is required for NHEJ independently of DNA termini complexity. (**A**) Inefficient REMI of plasmid DNA with non-compatible DNA ends into the genome of *Dictyostelium*. Ax2 cells were transfected with vector bearing two *Bam*HI or two *Pst*I termini in either the absence or presence of *Bam*HI. Following selection, blasticidin-resistant colonies were scored and REMI efficiency calculated for each strain as fold induction in the number of blasticidin-resistant colonies achieved by addition of *Bam*HI. Data are represented as the percentage induction of a given transfection relative to that achieved with the *Bam*HI cut vector. Error bars represent s.e.m. from three independent experiments. (**B**) Efficient REMI of plasmid DNA with one non-compatible and one compatible DNA end. Ax2 cells were transfected with vector bearing one *Bam*HI and one *Kpn*I overhang, either with or without 5′ phosphate groups having been removed by calf intestinal phosphatase (CIP), in the absence or presence of *Bam*HI as indicated. DNA termini introduced into cells are illustrated in the left-hand panel. Following selection, blasticidin-resistant colonies were scored. REMI efficiency was determined as in A. Data are represented as the percentage induction of a given transfection relative to that achieved with the *Bam*HI cut vector. Error bars represent s.e.m. from three independent experiments. (**C**) REMI of plasmid DNA with one non-compatible DNA end is dependent on NHEJ. Ax2, *dnapkcs*$^{-}$ or *ku80*$^{-}$ cells were transfected with vector bearing one *Bam*HI and one *Kpn*I overhang, both lacking 5′ phosphate groups, in either the absence or presence of *Bam*HI. Following selection, blasticidin-resistant colonies were scored. REMI efficiency was determined as in A. Data is represented as the percentage induction of a given strain relative to the parental Ax2 strain. Error bars represent s.e.m. from three independent experiments. (**D**) Parental Ax2 or *dclre1*$^{-}$ cells were transfected with plasmid DNA containing a *Bam*HI site at one end in combination with a 4-nucleotide 3′ overhang (*Kpn*I), 20-nucleotide 3′ overhang or hairpin structure at the other end, as indicated. Following selection, blasticidin-resistant colonies were scored for each transfection. REMI efficiency was calculated for each strain as fold induction in the number of blasticidin-resistant colonies achieved on addition of *Bam*HI to transfections. Data are represented as the percentage induction of a given strain relative to the parental Ax2 strain. Error bars represent s.e.m. from three independent experiments.

we observed no gross sensitivity of vegetative *dclre1*$^{-}$ cells to bleomycin (Fig. 4A). Although this might suggest an inactive NHEJ pathway in these cells, during the course of these experiments we noticed that *dclre1*$^{-}$ cells consistently showed delayed resumption of growth following bleomycin treatment when compared with Ax2 cells. To assess this further, we examined the ability of parental Ax2 and *dclre1*$^{-}$ cells to recover from transient exposure to DNA DSBs administered during vegetative cell growth. Exposure of Ax2 cells to bleomycin induces an arrest in cell growth, presumably through activation of a cell cycle checkpoint, with eventual expansion of cultures between 30 and 45 hours following removal of bleomycin (Fig. 4B). The *dclre1*$^{-}$ strain exhibits a similar arrest of cell growth following administration of DSBs (Fig. 4B). However, although Ax2 and *dclre1*$^{-}$ cells exhibit similar growth rates in the absence of bleomycin, *dclre1*$^{-}$ cells exhibit an extended delay in recovery following a transient exposure to DSBs (Fig. 4B; supplementary material Fig. S1). Importantly, *dclre1*$^{-}$ cells do not exhibit differential sensitivity to bleomycin (Fig. 4A) compared with Ax2 controls, implying that the observed extension of bleomycin-induced growth arrest is not due to increased cell death within the *dclre1*$^{-}$ culture, but might instead reflect a reduced ability to repair DNA damage.

The histone variant H2AX is phosphorylated in response to DSB (termed γ-H2AX) and decay of this signal is a commonly used marker for DSB repair (e.g. Goodarzi et al., 2008; Riballo et al., 2004). H2AX phosphorylation is conserved in *Dictyostelium* (Hudson et al., 2005). Therefore, to test whether the delay in resumption of cell growth in *dclre1*$^{-}$ cells is due to decreased efficiency of DSB repair in these cells, we compared decay of γ-H2AX in *dclre1*$^{-}$ and Ax2 cells. H2AX phosphorylation occurs rapidly in Ax2 and *dclre1*$^{-}$ cells (Fig. 4C) and, similar to other organisms, nuclear γ-H2AX foci become apparent throughout the

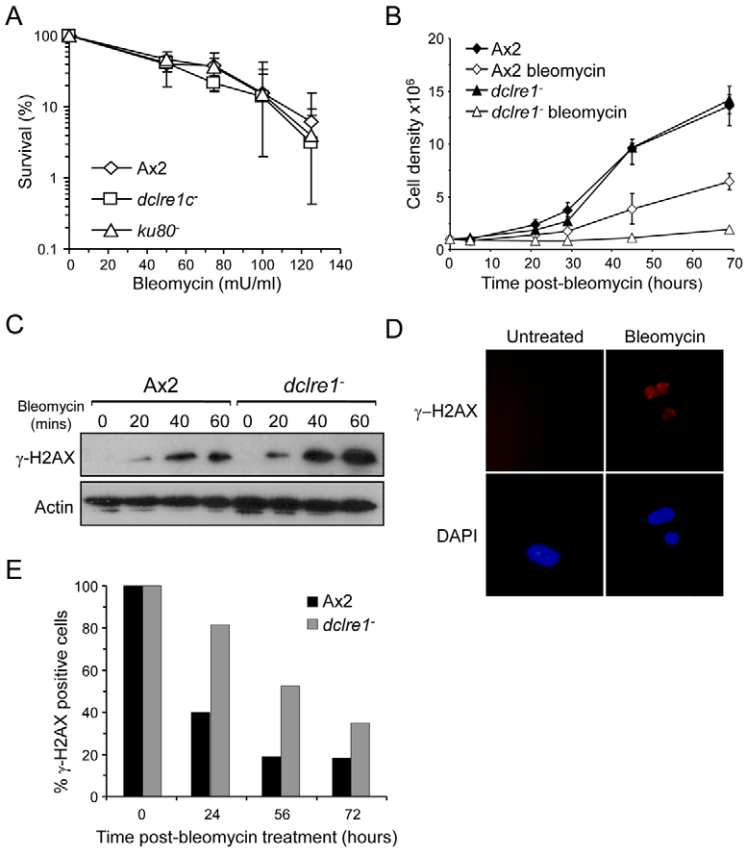

Fig. 4. Dclre1 is required for repair of DNA DSBs. (**A**) Exponentially growing Ax2, *dclre1*⁻ and *ku80*⁻ cells were exposed to increasing concentrations of bleomycin as indicated and cell survival assessed as described in the Materials and Methods. Error bars represent the s.e.m. from three independent experiments. (**B**) Cells were exposed to bleomycin at a concentration of 100 mU/ml for 1 hour. Following removal of bleomycin, cell density was determined at the indicated time points. Each point represents the s.e.m. of three replicates from a single experiment. One experiment representative of more than five is shown. (**C**) Ax2 or *dclre1*⁻ cells were exposed to 100 mU/ml bleomycin. Whole-cell extracts were prepared at 0, 20, 40 and 60 minutes following administration of DNA damage and subjected to western blotting with the indicated antibodies. (**D**) Ax2 cells were left untreated or exposed to 100 mU/ml bleomycin. Samples were fixed as described in the Materials and Methods, and subjected to immunofluorescence using the indicated antibody or DNA visualised using DAPI. (**E**) Ax2 or *dclre1*⁻ cells were exposed to 100 mU/ml bleomycin for 1 hour. At the indicated time points following removal of bleomycin, cells were stained with antibodies raised against γ-H2AX and subjected to immunofluorescence. The percentage γ-H2AX-positive cells were scored from a population of >200 cells. One experiment is shown, representative of more than three.

nucleus following exposure to DNA DSBs (Fig. 4D; supplementary material Fig. S2). Levels of γ-H2AX following damage are slightly elevated in the *dclre1*⁻ strain (Fig. 4C), suggesting an inability of these cells to resolve DNA damage compared with Ax2 controls. In this regard, the majority of Ax2 cells are no longer γ-H2AX positive 56 hours following removal of bleomycin, indicating repair of DNA damage. By contrast, γ-H2AX foci persist in *dclre1*⁻ cells, indicating a reduced ability to repair DSBs (Fig. 4E). A possible explanation for these observations is that, in addition to being required for NHEJ, Dclre1 is also required for HR and that the observed defect in recovery from DSBs in *dclre1*⁻ cells is a consequence of loss of this pathway. However, targeted integration efficiency at the *cdk8* locus is equivalent in Ax2 and *dclre1*⁻ cells, illustrating that *dclre1*⁻ cells are proficient in HR (Fig. 5B). Therefore, the observed DSB repair defect in *dclre1*⁻ cells reflects a reduced ability to repair DNA damage by an HR-independent mechanism. Given the decreased REMI in *dclre1*⁻ cells (Fig. 4), this is most likely through a compromised NHEJ pathway.

Deletion of *ku80* promotes HR and suppresses the DNA repair defect of *dclre1*⁻ cells

Given that disruption of *dclre1* results in a delay in DSB repair, we wished to establish whether loss of other NHEJ components results in a similar phenotype. In particular, given that Ku is required for recruitment of NHEJ factors to DSBs, we assessed the impact of disrupting this protein complex on DNA repair. Surprisingly, whereas *dclre1*⁻ cells exhibit delayed recovery from exposure to bleomycin, *ku80*⁻ cells recover from DSBs with kinetics similar to that of Ax2 cells (Fig. 5A). These data suggest that, in contrast to disruption of *dclre1*, loss of Ku has little impact on the ability of cells to repair DSBs. Consistent with this hypothesis, decay of γ-H2AX foci following administration of bleomycin to *ku80*⁻ cells is comparable to that observed in parental Ax2 controls (Fig. 5A).

These observations suggest that, in the absence of Ku, other pathways are able to restore genome integrity following DSBs. Loss of Ku in human cells promotes an alternative subpathway of NHEJ termed microhomology-mediated end joining (MMEJ), or alternative NHEJ (A-NHEJ), which involves limited resection of DNA termini to reveal short sequences of homology that are utilised for repair (Fattah et al., 2010; McVey and Lee, 2008). However, A-NHEJ will equally be able to promote integration of plasmid DNA into the genome of cells. Therefore, the inability of *ku80*⁻ cells to perform REMI would argue against an alternative end-joining pathway being responsible for efficient recovery from DSBs. Alternatively, loss of Ku in yeast and vertebrates renders DNA termini more susceptible to resection and promotes HR (Lee et al., 1998; Liang and Jasin, 1996). In this regard, whereas HR remains largely unaffected by deletion of *dclre1*, HR targeted at the *cdk8* locus is elevated in *ku80*⁻ cells (Fig. 5B). Taken together, these data suggest that, in the absence of Ku, DSBs are repaired more efficiently by HR. One prediction of this model is that deletion of *ku80* will suppress the DNA repair defect of *dclre1*⁻ cells. To test this, we generated a *dclre1*⁻*ku80*⁻ strain and assessed its ability to repair bleomycin-induced DNA DSBs. Similar to *ku80*⁻ and *dclre1*⁻ cells, the *dclre1*⁻*ku80*⁻ strain exhibits reduced REMI efficiency (supplementary material Fig. S3). Whereas *dclre1*⁻ cells exhibit the characteristic delay in γ-H2AX foci decay and cell growth following bleomycin treatment, this is not observed in the *dclre1*⁻*ku80*⁻ strain. Indeed, recovery from DSBs is slightly faster in these cells when compared with either Ax2 or *ku80*⁻ cells (Fig.

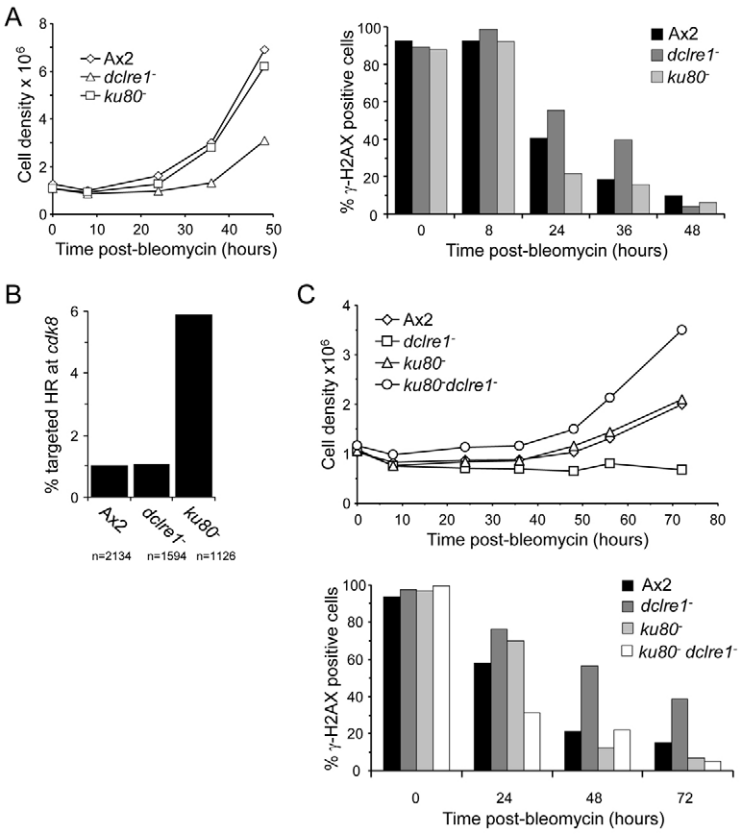

Fig. 5. Deletion of *ku80* suppresses the repair defect of *dclre1*$^{-}$ cells and promotes HR. (**A**) Ax2, *ku80*$^{-}$ and *dclre1*$^{-}$ cells were treated with 100mU/ml bleomycin for 1 hour. Following removal of bleomycin, cells were resuspended at a density of 1×10^{6} cells/ml in HL5. Cell density was determined at the indicated time points (left-hand panel). In parallel, cells were fixed, stained using antibodies raised against γ-H2AX and subjected to immunofluorescence. The percentage γ-H2AX-positive cells were scored from a population of >200 cells (right-hand panel). One experiment is shown, representative of at least three. (**B**) Ax2, *dclre1*$^{-}$ and *ku80*$^{-}$ cells were assessed for HR efficiency by measuring targeted integration of the blasticidin-resistance cassette at the *cdk8* locus. Multiple transfections were performed and drug-resistant clones were analysed for proper targeting by PCR. The percentage targeted HR at the *cdk8* locus is calculated as the proportion of aggregate-null colonies against the total number of colonies assessed. The *n* number represents the total number of clones analysed. (**C**) AX2, *dclre1*$^{-}$, *ku80*$^{-}$ and *ku80*$^{-}$*dclre1*$^{-}$ cells were treated with 100mU/ml bleomycin for 1 hour. Following removal of bleomycin, cells were resuspended at a density of 1×10^{6} cells/ml in HL5. Cell density was determined at the indicated time points (upper panel). In parallel, cells were fixed and stained using antibodies raised against γ-H2AX at the time points indicated. Cells that display γ-H2AX staining were identified by immunofluorescence. The percentage γ-H2AX-positive cells were scored from a population of >200 cells. One experiment is shown, representative of at least three.

5C). Therefore, deletion of Ku channels the repair of DSBs into alternative pathways other than NHEJ in vegetative *Dictyostelium*.

Discussion

Previously, we and others illustrated that *Dictyostelium* contains functional orthologues of DNA-PKcs and Ku that are required for resolution of DNA DSBs (Hudson et al., 2005; Muramoto and Chubb, 2008). Here, we further characterise their role in DSB repair by analysing the impact of disrupting these genes on REMI of DNA into the *Dictyostelium* genome. Although the stimulation of plasmid integration into the genome by co-transfection with restriction enzymes has been reported in a number of organisms (Kuspa and Loomis, 1992; Manivasakam et al., 2001; Schiestl and Petes, 1991), the molecular basis of this phenomenon remains unclear. REMI occurs independently of HR (Schiestl et al., 1994) and here we report that it is dependent on components of the NHEJ machinery in *Dictyostelium*. Furthermore, we exploit this assay to further illustrate conservation of the vertebrate NHEJ pathway in *Dictyostelium* by identifying a β-CASP-MBL family member with similarity to Artemis that is required for NHEJ.

To our knowledge, this is the first report of a β-CASP-MBL family member functioning in NHEJ outside vertebrates. Defects in human Artemis result in severe combined immunodeficiency due to a defect in processing DNA termini during V(D)J recombination (Moshous et al., 2001; Pannicke et al., 2004; Rooney et al., 2002). As Artemis is capable of processing complex DNA termini in vitro (Ma et al., 2002; Ma et al., 2005), these studies lead to speculation that this nuclease is required for processing a subset of complex DNA termini during NHEJ. However, our data illustrate that, although Dclre1 is required for NHEJ, this occurs independently of DNA end complexity. This highlights a requirement for Dclre1 beyond simple processing of DNA termini and suggests Artemis might similarly be required for aspects of NHEJ distinct from processing DNA ends. Indeed, although Artemis is required to repair a subset of potentially complex DSBs induced by IR (Darroudi et al., 2007; Riballo et al., 2004; Wang et al., 2005), more recent findings implicate this protein in facilitating NHEJ at sites close to or within heterochromatin independently of DNA termini complexity (Goodarzi et al., 2008). The assay employed here to assess NHEJ, in contrast to the usual plasmid repair assays employed in other systems, takes place in a chromatin context on one side of the break and could function in both heterochromatic and euchromatic regions of the genome. Given the genetic tractability of *Dictyostelium*, in addition to the similarity of *Dictyostelium* chromatin-modifying enzymes to those in humans (Chubb et al., 2006), it will be interesting to exploit *Dictyostelium* to assess the requirements for *dclre1* and other factors to facilitate integration of plasmid DNA into the genome in different chromatin contexts.

Although it is clear that *Dictyostelium* utilises components of the NHEJ machinery hitherto thought to be conserved only in vertebrates, to date it has not been exploited extensively to study DSB and other repair pathways. Consequently, little is know about how this organism combats DSBs at different stages of its life cycle. Previously, we demonstrated a reliance on NHEJ to combat DSBs administered as cells germinate from spores (Block and Lees-Miller, 2005; Hsu et al., 2006; Hudson et al., 2005; Muramoto and Chubb, 2008). Here, we extend these studies to assess the contribution of HR and NHEJ to DSB repair during vegetative cell growth. We find that, similar to mutation of other NHEJ components (Block and Lees-Miller, 2005; Hsu et al., 2006; Hudson et al., 2005; Muramoto and Chubb, 2008), disruption of *dclre1*

does not sensitise vegetative cells to bleomycin, indicating that the NHEJ pathway is not required to maintain cell viability following DSBs in *Dictyostelium*. Instead, the radiosensitivity of *exo1*$^{-}$ cells illustrates that HR is required for this process. This is consistent with the cell cycle distribution of vegetative *Dictyostelium*, with the majority of cells being in G2 (Muramoto and Chubb, 2008; Weijer et al., 1984), a stage of the cell cycle that would support HR (Branzei and Foiani, 2008). Thus, it would appear that, similar to yeast, HR is the predominant pathway utilised to combat DSBs in vegetative *Dictyostelium*, at least as regards maintaining cell viability following DNA damage. These data also imply that HR is the predominant pathway by which DSBs are repaired during G2 in *Dictyostelium*, in marked contrast to vertebrate cells, which rely principally on NHEJ in G1 and G2 (Beucher et al., 2009; Deckbar et al., 2007; Rothkamm et al., 2003). The reliance of *Dictyostelium* on HR might go some way to explaining the relatively high efficiency of gene disruption by targeted HR in this organism compared with vertebrates and its high resistance to ionising radiation (Deering, 1968).

What is striking about our data, however, is that, although NHEJ is not required for resistance of vegetative *Dictyostelium* to DSBs, NHEJ is functioning in some respect to combat this variety of DNA damage during this phase of the life cycle. This conclusion is based on our observations that: REMI of plasmid DNA into the genome is dependent on components of the NHEJ pathway; and disruption of a factor required for NHEJ-mediated REMI (*dclre1*) results in a delay to the repair of DSBs administered to vegetative cells. Therefore, both HR and NHEJ are capable of repairing DSBs in vegetative *Dictyostelium*. Interestingly, in contrast to *dclre1*$^{-}$ cells, we observe that, although Ku80 is required for efficient NHEJ in vegetative *Dictyostelium*, recovery from DSBs is largely unaffected in *ku80*$^{-}$ cells. Ku80 has recently been implicated in recovery from DSBs and progression of vegetative *Dictyostelium* through mitosis (Muramoto and Chubb, 2008). Although this study seems to conflict with our observations, it should be noted that our studies assess recovery from DSBs at later time points than those analysed by Muramoto and Chubb. Studies in human cells reveal that the G2-M checkpoint is released prior to completion of DSB repair (Krempler et al., 2007). One potential explanation for these discrepancies is that, although Ku is required for maintenance of G2-M arrest, *ku80*$^{-}$ cells do eventually pass through this checkpoint with persistent DSBs that are resolved in the subsequent cell cycle. This is a particularly attractive hypothesis given that DSBs will probably be repaired by HR in the subsequent S-G2 and that *ku80*$^{-}$ cells exhibit elevated levels of recombination (Fig. 5B). In both studies, however, a crucial role for Ku in facilitating DSB repair during G2 phase of the cell cycle is apparent.

The experiments described here do not directly assess whether NHEJ and HR are attempted at the same DSB in G2, or whether they function independently of each other at breaks with different end complexities or in different chromatin contexts. However, it should be noted that, although *dclre1*$^{-}$ cells show delayed recovery from DSBs, they do eventually repair damage and resume cell growth, an observation that is reflected in the lack of sensitivity of these cells to DSBs. A possible interpretation of these data is that NHEJ is attempted at a DSB first and, if unsuccessful, another repair pathway such as HR subsequently repairs DNA damage. For example, the delay in recovery from DSBs in *dclre1*$^{-}$ cells might reflect recognition of DNA ends by Ku and an unsuccessful attempt to perform NHEJ. In this regard, Ku rapidly binds DSBs before components of the HR machinery in vertebrate cells (Kim et al., 2005) and has been proposed to protect DNA termini from resection and inhibit HR in a number of different organisms (Barlow et al., 2008; Clerici et al., 2008; Lee et al., 1998; Liang and Jasin, 1996; Pierce et al., 2001; Wu et al., 2008; Zhang et al., 2007). A prediction of this model would be that a failure to initiate NHEJ would suppress defects in 'downstream' components of this pathway. Consistent with this, we find that deletion of Ku promotes HR and rescues the delay in DNA repair seen in *dclre1*$^{-}$ cells. Taken together, these data illustrate that both NHEJ and HR are active in vegetative *Dictyostelium* and highlight a role for Ku in determining DSB repair pathway choice in this organism.

Materials and Methods

Cell culture and strain generation

All strains were grown in association with *Klebsiella aerogenes* on SM agar or axenically using standard procedures.

To generate the *dclre1c*$^{-}$ disruption strain, fragments either upstream (nucleotides –865 to –155) or downstream (nucleotides +3078 to +3852) of the *dclre1*$^{-}$ gene (relative to A of the initiating ATG codon as +1 and T of the TGA stop codon as +3019) were amplified from Ax2 genomic DNA by PCR. These fragments were cloned either side of a blasticidin-resistance cassette contained in the pLPBLP plasmid (Faix et al., 2004; Sutoh, 1993) using *Kpn*I-*Hin*dIII for the upstream and *Pst*I-*Bam*HI for the downstream fragment. The resulting disruption construct was designed to delete the entire *dclre1*$^{-}$ gene. Transfection was carried out and cells subjected to selection with 10 μg/ml blasticidin the following day. Disrupted strains were isolated using standard procedures and confirmed by PCR.

To generate the *exo1*$^{-}$ disruption strain, fragments upstream (nucleotides –921 to –48) or downstream (nucleotides +1990 to +2474) of the *exo1*$^{-}$ gene (relative to A of the initiating ATG codon as +1) were amplified from Ax2 genomic DNA by PCR. These fragments were cloned either side of a blasticidin-resistance cassette contained within pLPBLP using *Kpn*I-*Hin*dIII for the upstream or *Eco*RV-*Pst*I for the downstream fragment. Transfection, selection and screening of strains disrupted in *exo1* were performed as described above.

To remove the blasticidin-resistance cassette from *ku80*$^{-}$, *dnapkcs*$^{-}$ and *dclre1*$^{-}$ cells, the relevant strains were transformed with plasmid pDEX-NLS-cre to express Cre recombinase. Blasticidin-sensitive clones were identified as described by Faix et al. (Faix et al., 2004) and verified for removal of the cassette by PCR. Generation of *ku80*$^{-}$*dclre1*$^{-}$ cells was achieved as above using the *dclre1* disruption vector in *ku80*$^{-}$ cells in which the BSR cassette had been removed.

Generation of expression constructs containing full-length Ku80 or Ku80 lacking the C-terminal DNA-PKcs interaction domain was achieved by amplifying the entire *ku80* gene including the stop codon (nucleotides +1 to 2511 relative to the A of the initiating ATG codon) or the *ku80* gene lacking the C-terminal 14 codons from Ax2 genomic DNA. A *Kpn*I restriction site and Myc tag were incorporated into the primer complementary to the N-terminus of the open reading frame, and an *Xba*I site was incorporated into the primer complementary to the C-terminal primer. The Myc–Ku80 sequences were subsequently placed under control of a constitutive promoter by cloning into the pDXA vector through the *Kpn*I and *Xba*I sites. Vectors were transfected into the relevant strain along with the helper plasmid pREP and transformants selected in G418.

Restriction-enzyme-mediated integration of plasmid DNA into the *Dictyostelium* genome

To generate vectors bearing restriction enzyme sites at their ends, a vector containing a blasticidin cassette (pLPBLP) (Faix et al., 2004) was cut with combinations of the appropriate restriction enzymes and treated with calf intestinal alkaline phosphatase where stated using standard procedures. DNA was purified by phenol extraction and ethanol precipitation prior to being used in transfections.

To generate vectors with a 20-nucleotide 3′ overhang or hairpin ends, adaptor oligonucleotides (see below) were ligated to one end of pLPBLP. The pLPBLP vector was cut with *Sal*I and the 5′ phosphate groups removed using CIP to prevent re-circularisation of the vector. Linearised pLPBLP was ligated to the appropriate adaptor oligonucleotide bearing a compatible *Xho*I end. The products were then digested with *Bam*HI to provide a compatible terminus at the opposite end of the vector. The final products were resolved by agarose gel electrophoresis and the fragments containing the ligated oligonucleotides identified by a shift in their mobility upon electrophoresis. The relevant fragments were isolated from gels and recovered using a QIAGEN gel extraction kit.

Sequences of the oligonucleotide adaptors are illustrated below. Underlined nucleotides indicate the *Xho*I site generated after annealing to the partner oligonucleotides (20-nucleotide 3′ overhang) or the counterpart sequence in the same oligonucleotide (hairpin).

20-nucleotide 3′ overhang: 5′-TCGAGAGTCCTACAGAAGGATCCCCC-CCCCCCCCCCCCCCCC-3′ and 5′-GATCCTTCTGTAGGACT-3′;

Hairpin: 5′-<u>TCGAG</u>AGTCCTACAGAAGGATCGATCCTTCTGTAGGACT<u>C</u>-3′).

Equal molar ratios of the oligonucleotides were mixed and heated at 95°C for 20 minutes and then cooled to room temperature to allow annealing.

REMI was performed as previously described (Kuspa and Loomis, 1992). Following electroporation, cells were resuspended in HL5 at 5×10^6 cells/ml and incubated at 22°C without shaking for 16 hours. Electroporated cells were spread on a 140 mm LPB agar plate (2.92 mM lactose, 0.1% bactopeptone, 19 mM Na_2HPO_4, 30 mM KH_2PO_4 and 2% agar) containing 10 μg/ml blasticidin in conjunction with 150 μl *E. coli B/r* resuspended in KK2 at an OD_{600} of 0.2–0.4. Blasticidin-resistant plaques were scored after 3 and 4 days.

Sensitivity of strains to DNA damage

Exponentially growing *Dictyostelium* cells were harvested and resuspended at a density of 5×10^6 cells/ml in 1 part HL5 to 5 parts KK2. Bleomycin sulfate (Sigma) was added to cells at the indicated concentrations in shaking suspension (160 rpm at 22°C) for one hour before dilution in KK2 to a density of 1×10^4 cells/ml. Replicates of 200 cells were plated on 15 cm SM agar plates in association with *K. aerogenes*. Survival was judged by plaque formation 3 and 4 days after plating.

Immunofluorescence

Exponentially growing *Dictyostelium* were harvested and resuspended at a density of 5×10^6 cells/ml in 1 part HL5 to 5 parts KK2. Bleomycin sulfate (Sigma) was added to a final concentration of 100 mU/ml in shaking suspension (100 rpm at 22°C) for one hour. Cells were washed three times with HL5 before resuspension at a density of 1×10^6 cells/ml in HL5 with shaking (100 rpm at 22°C). 1×10^6 cells were removed at the time points indicated and left to adhere to polylysine-coated cover slips for 5–10 minutes prior to incubation in pre-extraction buffer (10 mM PIPES pH 6.8, 300 mM sucrose, 3 mM $MgCl_2$, 20 mM NaCl, 0.5% Triton X-100) for 5 minutes. Cells were washed in Tris-buffered saline (TBS) and fixed for 5 minutes in 70% ethanol. After removal of ethanol, cover slips were washed once in ice-cold methanol, twice in TBS and blocked with 10% swine serum in TBS for 1 hour. Samples were subsequently incubated for 1 hour with anti-γ-H2AX (Abcam) diluted in blocking solution and washed three times with TBS before incubation for 1 hour with anti-rabbit TRITC (DAKO) diluted in blocking solution. Cover slips were washed three times with TBS and mounted using Vectorshield containing DAPI (Vector Labs). Immunofluorescence was detected using an Axioscope 2 fluorescent microscope equipped with Axiovision imaging software (Zeiss).

Cell proliferation following treatment with bleomycin

Exponentially growing *Dictyostelium* cells were harvested and resuspended at a density of 5×10^6 cells/ml in 1 part HL5 to 5 parts KK2. Bleomycin sulfate (Sigma) was added to a final concentration of 100 mU/ml in shaking suspension (100 rpm at 22°C) for one hour. Cells were washed three times with HL5 and resuspended at a density of 1×10^6 cells/ml in HL5. Cell density was determined microscopically at the indicated time points. At least two independent clones of a given strain were analysed for a phenotype.

Targeted HR efficiency at the *cdk8* locus

The *cdk8* knockout plasmid (Lin et al., 2004) was digested with *Kpn*I and *Not*I to liberate a fragment of DNA containing regions homologous to the *D. discoideum cdk8* gene flanking either the *BsR* or hygromycin-resistance cassettes, and purified using standard procedures.

Cells in the exponential phase of growth were transfected with 7 μg DNA using standard procedures, serial diluted in HL5 following a short recovery period and plated out in 96-well plates. After 24 hours, 10 μg/ml blasticidin was added and plates incubated in the dark at 22°C for 14 days. Following selection, clonal suspensions of blasticidin-resistant transformants were spotted onto SM-agar containing a lawn of *K. aerogenes*. After 5–6 days, plaques were large enough for phenotypic analysis. Targeted integration at the *cdk8* locus is indicated by an aggregation-defective phenotype. Targeted disruption of the *cdk8* locus only in aggregation-deficient colonies was confirmed by PCR analysis of genomic DNA isolated from randomly selected colonies.

To perform the HR assay in the *exo1*$^-$ strain, the *cdk8* knockout vector was modified to confer resistance to hygromycin. This was achieved by cutting the *cdk8* knockout vector with *Bam*HI to remove the *BsR* cassette and replacing it with the *Bam*HI-excised hygromycin-resistance cassette from the pHygTm(plus)/pG7 vector (a kind gift from Jeffrey Williams, University of Dundee, Scotland). Cells were transfected and subjected to selection with 40 μg/ml hygromycin the next day. Phenotypic analysis of hygromycin-resistant colonies was performed after 14 days as described above.

We are grateful to the curators of dictyBase (dictybase.org) for assistance. This work was supported by Cancer Research UK (www.cancerresearch.org.uk; grant C1521/A8182), the BBSRC (www.bbsrc.ac.uk; grant BBS/B/08051) and the Oxford University Clarendon Scholarship Fund.

Supplementary material available online at
http://jcs.biologists.org/cgi/content/full/124/10/1655/DC1

References

Barlow, J. H., Lisby, M. and Rothstein, R. (2008). Differential regulation of the cellular response to DNA double-strand breaks in G1. *Mol. Cell* **30**, 73-85.

Beucher, A., Birraux, J., Tchouandong, L., Barton, O., Shibata, A., Conrad, S., Goodarzi, A. A., Krempler, A., Jeggo, P. A. and Lobrich, M. (2009). ATM and Artemis promote homologous recombination of radiation-induced DNA double-strand breaks in G2. *EMBO J.* **28**, 3413-3427.

Block, W. D. and Lees-Miller, S. P. (2005). Putative homologues of the DNA-dependent protein kinase catalytic subunit (DNA-PKcs) and other components of the non-homologous end joining machinery in *Dictyostelium discoideum*. *DNA Repair (Amst.)* **4**, 1061-1065.

Boulton, S. J. and Jackson, S. P. (1996). *Saccharomyces cerevisiae* Ku70 potentiates illegitimate DNA double-strand break repair and serves as a barrier to error-prone DNA repair pathways. *EMBO J.* **15**, 5093-5103.

Branzei, D. and Foiani, M. (2008). Regulation of DNA repair throughout the cell cycle. *Nat. Rev. Mol. Cell Biol.* **9**, 297-308.

Chen, G., Shaulsky, G. and Kuspa, A. (2004). Tissue-specific G1-phase cell-cycle arrest prior to terminal differentiation in *Dictyostelium*. *Development* **131**, 2619-2630.

Chubb, J. R., Bloomfield, G., Xu, Q., Kaller, M., Ivens, A., Skelton, J., Turner, B. M., Nellen, W., Shaulsky, G., Kay, R. R. et al. (2006). Developmental timing in *Dictyostelium* is regulated by the Set1 histone methyltransferase. *Dev. Biol.* **292**, 519-532.

Clerici, M., Mantiero, D., Guerini, I., Lucchini, G. and Longhese, M. P. (2008). The Yku70-Yku80 complex contributes to regulate double-strand break processing and checkpoint activation during the cell cycle. *EMBO Rep.* **9**, 810-818.

Darroudi, F., Wiegant, W., Meijers, M., Friedl, A. A., van der Burg, M., Fomina, J., van Dongen, J. J., van Gent, D. C. and Zdzienicka, M. Z. (2007). Role of Artemis in DSB repair and guarding chromosomal stability following exposure to ionizing radiation at different stages of cell cycle. *Mutat. Res.* **615**, 111-124.

Deckbar, D., Birraux, J., Krempler, A., Tchouandong, L., Beucher, A., Walker, S., Stiff, T., Jeggo, P. and Lobrich, M. (2007). Chromosome breakage after G2 checkpoint release. *J. Cell Biol.* **176**, 749-755.

Deering, R. A. (1968). *Dictyostelium discoideum*: a gamma-ray resistant organism. *Science* **162**, 1289-1290.

DeFazio, L. G., Stansel, R. M., Griffith, J. D. and Chu, G. (2002). Synapsis of DNA ends by DNA-dependent protein kinase. *EMBO J.* **21**, 3192-3200.

Faix, J., Kreppel, L., Shaulsky, G., Schleicher, M. and Kimmel, A. R. (2004). A rapid and efficient method to generate multiple gene disruptions in *Dictyostelium discoideum* using a single selectable marker and the Cre-loxP system. *Nucleic Acids Res.* **32**, e143.

Falck, J., Coates, J. and Jackson, S. P. (2005). Conserved modes of recruitment of ATM, ATR and DNA-PKcs to sites of DNA damage. *Nature* **434**, 605-611.

Fattah, F., Lee, E. H., Weisensel, N., Wang, Y., Lichter, N. and Hendrickson, E. A. (2010). Ku regulates the non-homologous end joining pathway choice of DNA double-strand break repair in human somatic cells. *PLoS Genet.* **6**, e1000855.

Freim, J. O., Jr and Deering, R. A. (1970). Ultraviolet irradiation of the vegetative cells of *Dictyostelium discoideum*. *J. Bacteriol.* **102**, 36-42.

Goodarzi, A. A., Noon, A. T., Deckbar, D., Ziv, Y., Shiloh, Y., Lobrich, M. and Jeggo, P. A. (2008). ATM signaling facilitates repair of DNA double-strand breaks associated with heterochromatin. *Mol. Cell* **31**, 167-177.

Hsu, D. W., Gaudet, P., Hudson, J. J., Pears, C. J. and Lakin, N. D. (2006). DNA damage signaling and repair in *Dictyostelium discoideum*. *Cell Cycle* **5**, 702-708.

Hudson, J. J., Hsu, D. W., Guo, K., Zhukovskaya, N., Liu, P. H., Williams, J. G., Pears, C. J. and Lakin, N. D. (2005). DNA-PKcs-dependent signaling of DNA damage in *Dictyostelium discoideum*. *Curr. Biol.* **15**, 1880-1885.

Jackson, S. P. (2002). Sensing and repairing DNA double-strand breaks. *Carcinogenesis* **23**, 687-696.

Katz, K. S. and Ratner, D. I. (1988). Homologous recombination and the repair of double-strand breaks during cotransformation of *Dictyostelium discoideum*. *Mol. Cell. Biol.* **8**, 2779-2786.

Kim, J. S., Krasieva, T. B., Kurumizaka, H., Chen, D. J., Taylor, A. M. and Yokomori, K. (2005). Independent and sequential recruitment of NHEJ and HR factors to DNA damage sites in mammalian cells. *J. Cell Biol.* **170**, 341-347.

Krempler, A., Deckbar, D., Jeggo, P. A. and Lobrich, M. (2007). An imperfect G2M checkpoint contributes to chromosome instability following irradiation of S and G2 phase cells. *Cell Cycle* **6**, 1682-1686.

Kuspa, A. and Loomis, W. F. (1992). Tagging developmental genes in *Dictyostelium* by restriction enzyme-mediated integration of plasmid DNA. *Proc. Natl. Acad. Sci. USA* **89**, 8803-8807.

Lee, S. E., Moore, J. K., Holmes, A., Umezu, K., Kolodner, R. D. and Haber, J. E. (1998). *Saccharomyces* Ku70, Mre11/Rad50, and RPA proteins regulate adaptation to G2/M arrest after DNA damage. *Cell* **94**, 399-409.

Liang, F. and Jasin, M. (1996). Ku80 deficient cells exhibit excess degradation of extrachromosomal DNA. *J. Biol. Chem.* **271**, 14405-14411.

Lieber, M. R., Lu, H., Gu, J. and Schwarz, K. (2008). Flexibility in the order of action and in the enzymology of the nuclease, polymerases, and ligase of vertebrate non-homologous DNA end joining: relevance to cancer, aging, and the immune system. *Cell Res.* **18**, 125-133.

Lin, H. H., Khosla, M., Huang, H. J., Hsu, D. W., Michaelis, C., Weeks, G. and Pears, C. (2004). A homologue of Cdk8 is required for spore cell differentiation in *Dictyostelium*. *Dev. Biol.* **271**, 49-58.

Ma, Y., Pannicke, U., Schwarz, K. and Lieber, M. R. (2002). Hairpin opening and overhang processing by an Artemis/DNA-dependent protein kinase complex in nonhomologous end joining and V(D)J recombination. *Cell* **108**, 781-794.

Ma, Y., Schwarz, K. and Lieber, M. R. (2005). The Artemis:DNA-PKcs endonuclease cleaves DNA loops, flaps, and gaps. *DNA Repair (Amst.)* **4**, 845-851.
MacWilliams, H., Doquang, K., Pedrola, R., Dollman, G., Grassi, D., Peis, T., Tsang, A. and Ceccarelli, A. (2006). A retinoblastoma ortholog controls stalk/spore preference in *Dictyostelium*. *Development* **133**, 1287-1297.
Mahaney, B. L., Meek, K. and Lees-Miller, S. P. (2009). Repair of ionizing radiation-induced DNA double-strand breaks by non-homologous end-joining. *Biochem. J.* **417**, 639-650.
Manivasakam, P., Aubrecht, J., Sidhom, S. and Schiestl, R. H. (2001). Restriction enzymes increase efficiencies of illegitimate DNA integration but decrease homologous integration in mammalian cells. *Nucleic Acids Res.* **29**, 4826-4833.
McVey, M. and Lee, S. E. (2008). MMEJ repair of double-strand breaks (director's cut): deleted sequences and alternative endings. *Trends Genet.* **24**, 529-538.
Meek, K., Gupta, S., Ramsden, D. A. and Lees-Miller, S. P. (2004). The DNA-dependent protein kinase: the director at the end. *Immunol. Rev.* **200**, 132-141.
Moshous, D., Callebaut, I., de Chasseval, R., Corneo, B., Cavazzana-Calvo, M., Le Deist, F., Tezcan, I., Sanal, O., Bertrand, Y., Philippe, N. et al. (2001). Artemis, a novel DNA double-strand break repair/V(D)J recombination protein, is mutated in human severe combined immune deficiency. *Cell* **105**, 177-186.
Muramoto, T. and Chubb, J. R. (2008). Live imaging of the *Dictyostelium* cell cycle reveals widespread S phase during development, a G2 bias in spore differentiation and a premitotic checkpoint. *Development* **135**, 1647-1657.
Pannicke, U., Ma, Y., Hopfner, K. P., Niewolik, D., Lieber, M. R. and Schwarz, K. (2004). Functional and biochemical dissection of the structure-specific nuclease ARTEMIS. *EMBO J.* **23**, 1987-1997.
Pierce, A. J., Hu, P., Han, M., Ellis, N. and Jasin, M. (2001). Ku DNA end-binding protein modulates homologous repair of double-strand breaks in mammalian cells. *Genes Dev.* **15**, 3237-3242.
Rajawat, J., Vohra, I., Mir, H. A., Gohel, D. and Begum, R. (2007). Effect of oxidative stress and involvement of poly(ADP-ribose) polymerase (PARP) in *Dictyostelium discoideum* development. *FEBS J.* **274**, 5611-5618.
Raynard, S., Niu, H. and Sung, P. (2008). DNA double-strand break processing: the beginning of the end. *Genes Dev.* **22**, 2903-2907.
Riballo, E., Kuhne, M., Rief, N., Doherty, A., Smith, G. C., Recio, M. J., Reis, C., Dahm, K., Fricke, A., Krempler, A. et al. (2004). A pathway of double-strand break rejoining dependent upon ATM, Artemis, and proteins locating to gamma-H2AX foci. *Mol. Cell* **16**, 715-724.
Rooney, S., Sekiguchi, J., Zhu, C., Cheng, H. L., Manis, J., Whitlow, S., DeVido, J., Foy, D., Chaudhuri, J., Lombard, D. et al. (2002). Leaky Scid phenotype associated with defective V(D)J coding end processing in Artemis-deficient mice. *Mol. Cell* **10**, 1379-1390.
Rothkamm, K., Kruger, I., Thompson, L. H. and Lobrich, M. (2003). Pathways of DNA double-strand break repair during the mammalian cell cycle. *Mol. Cell. Biol.* **23**, 5706-5715.
Schiestl, R. H. and Petes, T. D. (1991). Integration of DNA fragments by illegitimate recombination in *Saccharomyces cerevisiae*. *Proc. Natl. Acad. Sci. USA* **88**, 7585-7589.
Schiestl, R. H., Zhu, J. and Petes, T. D. (1994). Effect of mutations in genes affecting homologous recombination on restriction enzyme mediated and illegitimate recombination in *Saccharomyces cerevisiae*. *Mol. Cell. Biol.* **14**, 4493-4500.
Secretan, M. B., Scuric, Z., Oshima, J., Bishop, A. J., Howlett, N. G., Yau, D. and Schiestl, R. H. (2004). Effect of Ku86 and DNA-PKcs deficiency on non-homologous end-joining and homologous recombination using a transient transfection assay. *Mutat. Res.* **554**, 351-364.
Sutoh, K. (1993). A transformation vector for *Dictyostelium discoideum* with a new selectable marker bsr. *Plasmid* **30**, 150-154.
Wang, J., Pluth, J. M., Cooper, P. K., Cowan, M. J., Chen, D. J. and Yannone, S. M. (2005). Artemis deficiency confers a DNA double-strand break repair defect and Artemis phosphorylation status is altered by DNA damage and cell cycle progression. *DNA Repair (Amst.)* **4**, 556-570.
Weijer, C. J., Duschl, G. and David, C. N. (1984). A revision of the *Dictyostelium discoideum* cell cycle. *J. Cell Sci.* **70**, 111-131.
Wilson, S., Warr, N., Taylor, D. L. and Watts, F. Z. (1999). The role of *Schizosaccharomyces pombe* Rad32, the Mre11 homologue, and other DNA damage response proteins in non-homologous end joining and telomere length maintenance. *Nucleic Acids Res.* **27**, 2655-2661.
Wu, D., Topper, L. M. and Wilson, T. E. (2008). Recruitment and dissociation of nonhomologous end joining proteins at a DNA double-strand break in *Saccharomyces cerevisiae*. *Genetics* **178**, 1237-1249.
Zhang, X. Y., Langenick, J., Traynor, D., Babu, M. M., Kay, R. R. and Patel, K. J. (2009). Xpf and not the Fanconi anaemia proteins or Rev3 accounts for the extreme resistance to cisplatin in *Dictyostelium discoideum*. *PLoS Genet.* **5**, e1000645.
Zhang, Y., Hefferin, M. L., Chen, L., Shim, E. Y., Tseng, H. M., Kwon, Y., Sung, P., Lee, S. E. and Tomkinson, A. E. (2007). Role of Dnl4-Lif1 in nonhomologous end-joining repair complex assembly and suppression of homologous recombination. *Nat. Struct. Mol. Biol.* **14**, 639-646.

Journal of Cell Science

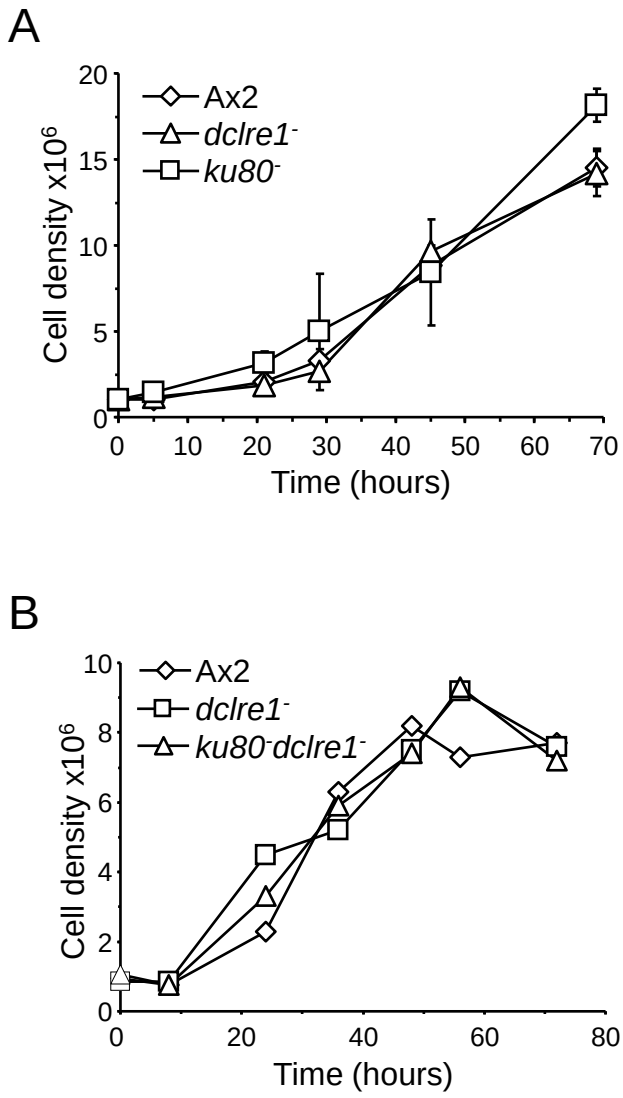

Fig. S1. Growth rate of strains in the absence of DNA damage.
A. Ax2, *dclre1*$^-$ or *ku80*$^-$ cells were seeded at a density of $1x10^6$ and cell density was determined at the indicated time points. Each point represents the SEM of 3 replicates.
B. Ax2, *dclre1*$^-$ or *ku80*$^-$*dclre1*$^-$ cells were seeded at a density of $1x10^6$ and cell density was determined at the indicated time points.

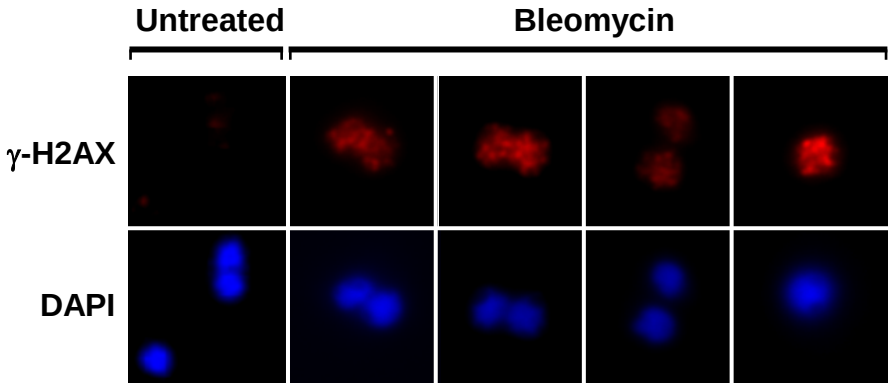

Supplementary Figure S2: DSB-induced nuclear staining for γ-H2AX.

Ax2 cells were left untreated or exposed to 100mU/ml of bleomycin for 1 hour. Cells were processed, stained with antibodies raised against γ-H2AX, and subjected to immunofluorescence as described in Materials and Methods. Several representative patterns of DSB-induced γ-H2AX staining are illustrated.

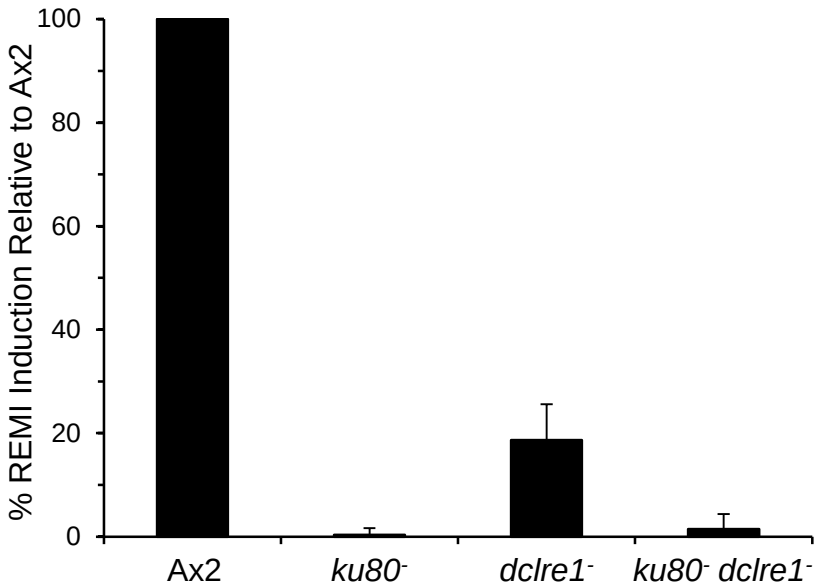

Fig. S3: REMI of plasmid DNA into *Dictyostelium* genome is defective in *ku80-dclre1-* cells.

Ax2, *ku80-*, *dclre1-* and *ku80-dclre1-* cells were transfected with *Bam*HI linearised vector containing a blasticidin resistant cassette either alone or in combination with *Bam*HI. Following selection, blasticidin resistant colonies were scored for each transfection and REMI efficiency calculated for each strain as fold induction in number of blasticidin resistant colonies achieved by addition of *Bam*HI. Data is represented as the % induction of a given strain relative to the parental Ax2 strain. Error bars represent standard error of the mean (SEM) from four independent experiments.